J Am Soc Nephrol 15: 928–939, 2004

The Parietal Epithelial Cell: A Key Player in the Pathogenesis of Focal Segmental Glomerulosclerosis in Thy-1.1 Transgenic Mice

BART SMEETS,* NATHALIE A.J.M. TE LOEKE,* HENRY B.P.M. DIJKMAN,* MARK L.M. STEENBERGEN,* JOOST F.M. LENSEN[‡], MARK P.V. BEGIENEMAN,* TOIN H. VAN KUPPEVELT,[‡] JACK F.M. WETZELS,[†] and ERIC J. STEENBERGEN*

*Departments of *Pathology, [†]Nephrology, and [‡]Biochemistry, University Medical Center Nijmegen, Nijmegen, the Netherlands.*

Abstract. Focal segmental glomerulosclerosis (FSGS) is a hallmark of progressive renal disease. Podocyte injury and loss have been proposed as the critical events that lead to FSGS. In the present study, the authors have examined the development of FSGS in Thy-1.1 transgenic (tg) mice, with emphasis on the podocyte and parietal epithelial cell (PEC). Thy-1.1 tg mice express the Thy-1.1 antigen on podocytes. Injection of anti-Thy-1.1 mAb induces an acute albuminuria and development of FSGS lesions that resemble human collapsing FSGS. The authors studied FSGS lesions at days 1, 3, 6, 7, 10, 14, and 21, in relation to changes in the expression of specific markers for normal podocytes (WT-1, synaptopodin, ASD33, and the Thy-1.1 antigen), for mouse PEC (CD10), for activated podocytes (desmin), for macrophages (CD68), and for proliferation (Ki-67). The composition of the extracellular matrix (ECM) that forms tuft adhesions or scars was studied using mAb against collagen IV α2 and α4 chains and antibodies directed against different heparan sulfate species. The first change observed was severe PEC injury at day 1, which increased in time, and resulted in denuded segments of Bowman's capsule at days 6 and 7. Podocytes showed foot process effacement and microvillous transformation. There was no evidence of podocyte loss or denudation of the GBM. Podocytes became hypertrophic at day 3, with decreased expression of ASD33 and synaptopodin and normal expression of WT-1 and Thy-1.1. Podocyte bridges were formed by attachment of hypertrophic podocytes to PEC and podocyte apposition against denuded segments of Bowman's capsule. At day 6, there was a marked proliferation of epithelial cells in Bowman's space. These proliferating cells were negative for desmin and all podocyte markers, but stained for CD10, and thus appeared to be PEC. The staining properties of the early adhesions were identical to that of Bowman's capsule, suggesting that the ECM in the adhesions was produced by PEC. In conclusion, the authors propose the following sequence of events leading to FSGS lesions in the Thy1.1 tg mice: (*1*) PEC damage and denudation of Bowman's capsule segments; (*2*) podocyte hypertrophy and bridging; and (*3*) PEC proliferation with ECM production.

Focal segmental glomerulosclerosis (FSGS), a hallmark of progressive renal disease, is one of the most common patterns of glomerular injury encountered in human renal biopsies (1). In its classical form, FSGS is characterized by mesangial sclerosis, obliteration of glomerular capillaries, formation of adhesions between the glomerular tuft and Bowman's capsule, podocyte hypertrophy, hyalinosis, and intracapillary foam cells. More recently, various morphologic variants have been described (2). Notably, FSGS is merely a descriptive diagnosis and not a disease entity. Clinically, presentation of the patients varies widely (3).

FSGS was long considered to be the consequence of mesangial overload leading to mesangial cell proliferation, mesangial cell injury, and increased production of extracellular matrix (ECM) (4–7). More recently, focus has turned on the visceral epithelial cell, the so-called podocyte. Seminal studies of Kriz *et al.* (8–17) in various rat models of FSGS have proposed the following sequence of events that ultimately lead to FSGS: (*1*) podocyte injury resulting in podocyte loss with denudation of the GBM; (*2*) adherence of the parietal epithelial cell (PEC) to the naked GBM; (*3*) formation of an adhesion of the GBM to Bowman's capsule; (*4*) misdirected filtration of proteins to the periglomerular and peritubular space. However, the studies by Kriz *et al.* were performed in animal models in which a common feature was glomerular hypertension with capillary ballooning and the development of hypocellular FSGS lesions, which resemble lesions observed in human secondary FSGS. Their findings may therefore not apply to FSGS in general. Recently, we have proposed the Thy-1.1 transgenic (tg) mice as a mouse model to study proteinuria and FSGS (18). Thy-1.1 tg mice carry a mouse-human chimeric transgene that causes ectopic expression of the mouse Thy-1.1 antigen on podocytes. Injection of mAb directed against the

Received August 15, 2003. Accepted January 21, 2004.
Correspondence to Dr. B. Smeets, Department of Pathology, University Medical Center Nijmegen, P.O. Box 9101, 6500 HB, Nijmegen, The Netherlands. Phone: 31-24-3614326; Fax: 31-24-3540520; E-mail: b.smeets@pathol.umcn.nl

1046-6673/1504-0928
Journal of the American Society of Nephrology

DOI: 10.1097/01.ASN.0000120559.09189.82

Thy-1.1 antigen induces an acute albuminuria within 10 min and a dose-dependent development of FSGS within 3 wk (19). FSGS lesions in this mouse model bear resemblance to the collapsing variant of human FSGS.

In the present study, we have examined the histopathologic changes that occur in the early stages of FSGS development. We particularly focused on the podocytes and PEC. Our results indicate that PEC play the principal role in the formation of FSGS lesions in this mouse model.

Materials and Methods

Animals

Heterozygous Thy-1.1 tg mice were kindly provided by Dr. D.J. Evans (T6, T-construct mice (20)). These mice were generated by injecting a hybrid human-mouse Thy-1.1 gene into pronuclei of zygotes of Thy-1.2 CBA × C57BL/10 mice. These mice express the Thy-1.1 gene abnormally in podocytes, resulting in the presence of the Thy-1.1 antigen on the podocytes. All mice were bred in our animal facility. Breading pairs consisted of a heterozygous (+/−) tg mouse and its non-tg (−/−) counterpart. The presence of the tg was examined by PCR on genomic DNA from the tail, with a forward primer: 5'-CGCCTGAGTCCTGATCTCC-3' and a reverse primer: 5'-AACCTGCATCTTCACTGGGT-3'. The presence of the tg resulted in a specific 834-bp amplicon. As a positive control for the presence of amplifiable genomic DNA, a primerset for aminopeptidase A (APA; EC 3.4.11.7), consisting of the forward primer: 5'-ACACAACCCCAGCTCCTTCC-3' and reverse primer 5'-TCTTCTGCAGCCTGGATCAC-3', was used. The amplification of the APA gene with these primers resulted in a 367-bp amplicon.

Anti-Thy-1.1 mAb

For *in vivo* experiments, a mouse anti-mouse Thy-1.1 mAb (19XE5: subclass IgG3) was used. 19XE5 was generated *in vitro*, by hollow fiber culture, purified by protein-A column affinity chromatography and concentrated (Nematology Department, Agriculture University Wageningen, The Netherlands). The mAb was decomplemented at 56°C for 45 min and sterilized by passage through a sterile 0.2-μm filter, and stored at −80°C.

Animal Experiments

Five-week-old Thy-1.1 tg mice received an intravenous injection with 1 mg anti-Thy-1.1 mAb (19XE5) in 0.1 ml 0.9% saline solution. Transgenic mice injected with 0.1 ml 0.9% saline solution alone were used as controls. To evaluate the FSGS development, kidney samples were collected at days 1, 3, 6, 7, 10, 14, and 21 after anti-Thy-1.1 mAb injection.

Light Microscopy and Transmission Electron Microscopy

For light microscopy, kidney fragments were fixed in Bouin solution, dehydrated, and embedded in paraplast (Amstelstad, Amsterdam The Netherlands). Four-micrometer sections were stained with periodic acid-Schiff, and 2-μm sections with silver methenamine (21). At least 60 glomeruli per mouse were evaluated. We determined the percentage of glomeruli with a FSGS lesion (FGS score). Only lesions with an adhesion (matrix continuity between the tuft and Bowman's capsule in the silver stain) were counted. The number of nuclei in Bowman's space was determined (expressed as nuclei/glomerular cross section) and served as an objective measure for hyperplasia of glomerular epithelial cells.

For electron microscopy, we used immersion and perfusion fixed kidneys. For immersion fixation, small fragments of cortex were fixed in 2.5% glutaraldehyde dissolved in 0.1 M sodium cacodylate buffer, pH 7.4, overnight at 4°C and washed in the same buffer. To obtain perfusion fixed kidneys, anti-Thy-1.1–injected mice were perfused retrogradely via the aorta. The animals were flushed for 30 s with a buffered saline solution and perfused with a 2.5% glutaraldehyde dissolved in 0.1 M sodium cacodylate buffer, pH 7.4, for 10 min. Perfusion was performed at a pressure of 120 mmHg. Small fragments of cortex were further fixed by immersion in the same fixative overnight at 4°C and washed in 0.1 M sodium cacodylate buffer, pH 7.4. The tissue fragments were postfixed in Palade-buffered 2% OsO4 for 1 h, dehydrated, and embedded in Epon812, Luft procedure (Merck, Darmstadt, Germany). Ultrathin serial sections with 2-μm intervals were contrasted with 4% uranyl acetate for 45 min and subsequently with lead citrate for 5 min at room temperature. Sections were examined in a Jeol 1200 EX2 electron microscope (JEOL, Tokyo, Japan).

Immunohistochemistry

Immunohistochemical staining was performed on kidneys, fixed in 4% buffered formaldehyde for 24 h and embedded in paraffin. Four-micrometer sections were incubated with rat rabbit anti-mouse Ki-67 (Dianova Immundiagnostic, Hamburg, Germany), goat anti-CD10, and rabbit anti-WT-1 (Santa Cruz Biotechnology, Santa Cruz, CA). As secondary antibodies we used, a biotinylated goat anti-rabbit antibody for Ki-67 and WT-1, and a horse anti-goat for CD10 (Vector laboratories Inc., Burlingame, CA). Detection was carried out with vectastain ABC kit (Vector Laboratories, Burlingame, CA) with the use of peroxidase as label and diaminobenzidine as substrate. Quantification of the WT-1 and Ki-67–positive cells was performed with the Zeiss KS 400 image analysis system (Carl Zeiss b.v., Weesp, The Netherlands). Images were acquired using AxioPlan2 imaging microscope and AxioCam MRc digital ccd camera (Carl Zeiss b.v., Weesp, The Netherlands). The outline of individual glomeruli and segments of interstitium were interactively drawn using a graphic tablet. Positive nuclei in the selected areas were interactively marked. A customized macro under KS400 software (KS400 3.0) determined the area (mm^2) of the selected segments, and the number of positive nuclei within this area. Approximately 30 glomeruli per mouse were counted in one cross-section. For staining of CD68 and desmin, we used 2-μm acetone fixed cryosections. The sections were incubated with rat anti-mouse CD68 (clone FA-11; Serotec, Oxford, UK), and rabbit anti-desmin (22). As secondary antibodies we used biotinylated rabbit anti-rat for CD68 and biotinylated goat anti-rabbit antibody for desmin (Vector laboratories Inc., Burlingame, CA). Detection was carried out with vectastain ABC kit for alkaline phophatase detection (Vector Laboratories, Burlingame, CA).

Immunofluorescence Microscopy

Kidney fragments were snap-frozen in liquid nitrogen, and 2-μm acetone fixed serial cryostat sections were used. Thy-1.1 was detected using a rat polyclonal anti-Thy-1 antibody (59AD2.2; IgG2a, (23)). As secondary antibody, we used a FITC-labeled sheep anti-rat antibody (Serotec, Oxford, UK). A double-immunolabeling technique was performed to determine the co-localization of Thy-1.1 and Ki-67 and of Thy1.1 and desmin. Thy-1.1 was stained as described above. After washing with PBS, the sections were incubated with rabbit anti-mouse Ki-67 (Dianova Immundiganostic, Hamburg Germany) or with rabbit anti-desmin (22) and detected with a goat anti-rabbit Alexa 568 antibody (Molecular Probes Inc, Leiden, The Netherlands). Syn-

aptopodin was detected using an anti-synaptopodin mAb (Progen Biotechnik, Heidelberg, Germany), followed by FITC-labeled sheep anti-mouse IgG1 (Nordic Immunologicals, Tilburg, The Netherlands). For detection of the podocyte, we also have used ASD33, a rat monoclonal antibody, generated in our laboratory, which only reacts with the podocyte cell membrane (24). The identity of the antigen is unknown. For the detection of ASD33, we have used FITC-labeled rabbit anti-rat antibody (Dako A/S, Glostrup, Denmark). Type IV collagen $\alpha 2$ and $\alpha 4$ chains were detected with rat monoclonal antibodies directed against human collagen (IV) $\alpha 2$ (H22) and human collagen (IV) $\alpha 4$ (H43), a gift from Dr. Yoshikazu Sado (Shigei Medical Research Institute, Okayama, Japan). Detection was done using goat anti-rat Alexa 488/568 antibodies (Molecular Probes Inc, Leiden, The Netherlands). Nuclei were stained with TO-PRO-3 (Molecular Probes Inc, Leiden, The Netherlands), a monomeric cyanine nucleic acid stain. Different heparan sulfate species were detected with various single chain antibodies, HS4C3 (25), HS4E4, and EV3C3 (26). The single chain antibodies were detected with a Cy3-labeled rabbit antibody directed against the VSV-g epitope tag (Sigma-Aldrich, Zwijndrecht, The Netherlands). The sections were examined with a confocal laser-scanning microscope (CLSM) (Leica lasertechnik GmbH, Heidelberg, Germany).

Statistical Analyses

For multiple comparisons, ANOVA was used and *post hoc* analyses were done with Tukey test. $P < 0.05$ was considered significant. All values are expressed as means ± SEM.

Results

Histopathology of the Kidney

Thy-1.1 tg mice that received a single injection of 1 mg anti-Thy-1.1 mAb developed FSGS lesions within 3 wk. The histopathology was examined by light microscopy at days 1, 3, 6, 7, 10, and 21 (Figure 1). At day 1, we observed enlarged Bowman's space due to collapse of the glomerular tuft, consistent with ischemia. No enlarged podocytes (hypertrophy) were observed. In contrast, PEC showed vacuolization and detachment. In tubular lumens we observed many hyaline appearing protein casts. Proximal tubular epithelial cells showed damage similar to PEC (Figure 1A). At day 3, glomeruli were not ischemic anymore, and the number of tubular protein casts had decreased. There was segmental hypertrophy of glomerular epithelial cells (Figure 1B). At days 6 and 7, the first FSGS lesions with tuft adhesions to Bowman's capsule were observed. Affected glomeruli showed segmental collapse of the capillary tuft and a marked increase of epithelial cells in Bowman's space (Figure 1, C and D). It was shown that there was a significant overall increase of the number of nuclei in bowman's space at day 7 (Table 1). Adhesions (continuity of ECM between the capillary tuft and Bowman's capsule) were formed by thin strands of ECM that were located in between the epithelial cells in Bowman's space. Sporadically (not quantified) we observed endocapillary foam cells, an endocapillary neutrophil or mononuclear cell, mild mesangial hypercellularity, and mild hyalinosis (Figure 1F). From a histologic point of view, the FSGS lesions closely resembled the collapsing variant of human FSGS (27). The percentage of glomeruli with FSGS lesions was scored at days 1, 3, 6, 7, 10, and 21 by light microscopy (Figure 1G). FSGS lesions, with tuft adhesions to Bowman's capsule, could be observed in 11 ± 1% and 26 ± 3% of the glomeruli at days 6 and 7, respectively. The percentage of glomeruli with FSGS lesions did not increase thereafter. However, at day 21, the lesions were more advanced, showing a high degree of ECM accumulation, which had culminated in the formation of segmental or even global scars (Figure 1E).

EM analysis at days 1 and 3, using immersion fixed tissue, showed global podocyte alterations with foot process effacement and microvillous transformation. However, we did not observe podocyte detachment or areas of denuded GBM. In contrast to humans, mouse glomeruli frequently show prominent intraglomerular proximal tubular epithelial cells. These "glomerular proximal tubular cells" and PEC showed extensive nuclear activation, vacuolization, and widespread injury especially at day 1 (Figure 2A). As most FSGS lesions develop around days 6 and 7, we performed extensive EM analysis at this time point, using both immersion and perfusion fixed tissue. At days 6 and 7, in early lesions, PEC appeared activated with enlarged nuclei and prominent nucleoli. The number of PEC nuclei along Bowman's capsule appeared increased, and mitotic figures were occasionally encountered (Figure 2, C and D). Detachment of PEC with naked BC was occasionally observed (Figure 2B). In affected glomerular segments, the podocytes were markedly hypertrophic, showing extensive vacuolization, resorption droplets, and formation of pseudocysts (Figure 2D). In immersion-fixed tissue, Bowman's space was absent and hypertrophic podocytes were positioned directly against PEC. In perfusion-fixed tissue, we frequently observed cell bridges formed by a hypertrophic podocyte attached to a PEC (in our hands perfusion fixation, as compared to immersion, leads to more shrinkage of the glomerular tuft and flattening of the PEC, resulting in a prominent Bowman's space). At the interface between hypertrophic podocytes and PEC, junctional complexes were occasionally observed (Figure 2E). In immersion-fixed tissue, we did occasionally see podocytes positioned directly against denuded Bowman's capsule (Figure 2B); in the perfusion-fixed tissue, optically empty space was always present and true attachment could not be confirmed. In more advanced lesions, Bowman's space was filled with an increased number of epithelial cells (both fixation techniques), and pericellular accumulation of matrix was observed (Figure 2F). Serial sections of single glomeruli showed that FSGS lesions did not develop exclusively close to the urinary pole but were also encountered near the vascular pole (Figure 2C).

Podocyte Phenotype

To assess changes in podocyte phenotype during the development of FSGS, we studied the expression of podocyte-specific markers, WT-1, synaptopodin, ASD33 (an unidentified cell membrane antigen, strongly expressed on mouse podocytes), the Thy-1.1 antigen, Ki-67 as a marker of proliferation, desmin (associated with podocyte dedifferentiation) (28), and CD68 (macrophage marker). At day 3, in the absence of sclerotic lesions, we already observed some decrease in the expression of ASD33 and synaptopodin (data not shown). At days 6 and 7, changes were even

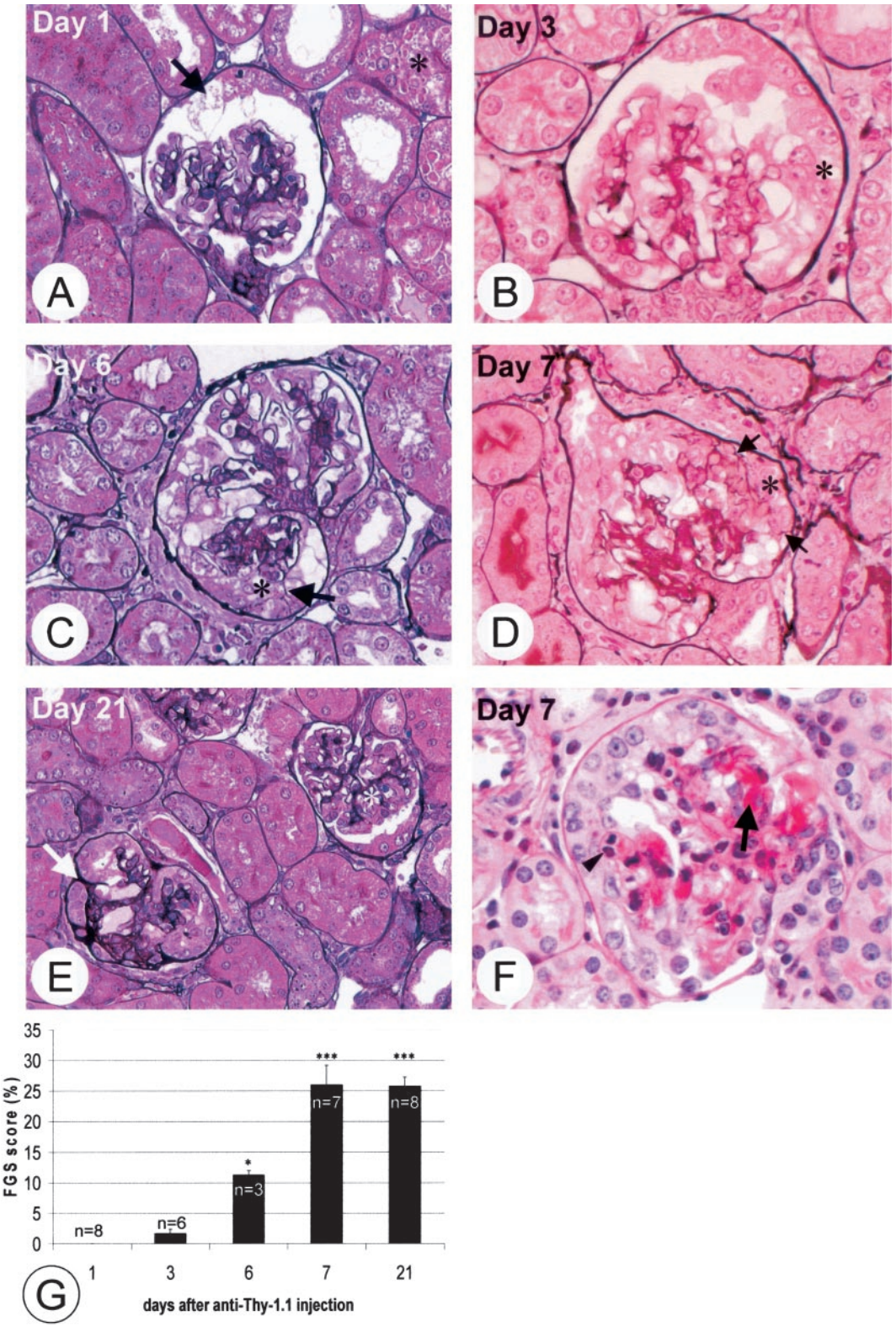

Figure 1. Histology of kidney sections of Thy-1.1 transgenic (tg) mice at days 1, 3, 6, 7, and 21 after anti-Thy-1.1 mAb injection, (A-E, respectively). (A) At day 1, light microscopy revealed vacuolization and detachment of PEC (arrow). In proximal tubules, many protein resorption droplets were observed (*). (B) At day 3, a pronounced hypertrophy of glomerular epithelial cells was observed (*). (C and D) At days 6 and 7, tuft adhesions were observed (arrows). Glomeruli showed segmental collapse of capillaries and an increased number of epithelial cells in Bowman's space (*). (E) At day 21, glomeruli showed accumulation of ECM in Bowman's space, with formation of segmental scars (arrow); unaffected glomerulus (*). Methenamine silver staining; original magnification, ×400. (F) Mild hyalinosis (arrow) and a mitotic endocapillary cell (arrowhead) were occasionally observed. PAS staining; original magnification, ×400. The percentage of glomeruli with FSGS lesions at days 1, 3, 6, 7, and 21 is depicted in panel G. * $P < 0.05$, *** $P < 0.001$ *versus* day 1.

more prominent (Figure 3A). The decrease of ASD33 and synaptopodin expression was particularly observed in segments with a tuft adhesion or tuft collapse. During the first 7 d, we did not observe a change in the number of WT-1–positive cells. At day 21, we did observe a significant decrease in number of WT-1–positive podocytes compared with days 1 and 6 (Table 2). At day 7, there was an increased expression of desmin in affected glomeruli. Desmin co-localized with the Thy-1,1 antigen and is expressed by podocytes (Figure 3B). There was no glomerular expression for CD68 (data not shown).

Table 1. Number of nuclei in the urinary space in Thy-1.1 tg mice at days 1 and 7 after anti-Thy-1.1 mAb injection and in saline injected mice[a]

Group	Number of Nuclei in Bowman's Space	*n*
Saline	15.7 ± 0.4	4
Day 1	14.7 ± 0.6	3
Day 7	19.5 ± 1.3[b]	4

[a] Significant increase in number of nuclei at day 7 after anti-Thy-1.1 injection *versus* the saline injected mice and mice at day 1 after anti-Thy-1.1 injection.

[b] $P < 0.05$ *versus* day 1 and saline.

Characterization of the Proliferating Epithelial Cells

We have performed phenotypic analysis of proliferating epithelial cells in Bowman's space to clarify their origin. Sections were stained for Ki-67. We observed an increase in the number of proliferating cells, which peaked at day 3 for the interstitial compartment and at day 7 for the glomerulus (approximately 5× baseline levels). Thereafter, the number of Ki-67–positive cells declined to baseline levels (Figure 4A). Approximately 50% of proliferating cells were located in Bowman's space; the rest were located within the glomerular tuft. Proliferating cells were often located adjacent to adhesions (Figure 5B). In addition, proliferating cells were often positioned along Bowman's capsule and appeared to be PEC (Figure 4B). By double immunofluorescence, we never observed co-localization of Ki-67 and the podocyte specific Thy-1.1 antigen, arguing against the presence of proliferating podocytes. We did not observe Thy-1.1 expression in areas with accumulations of epithelial cells in Bowman's space (Figure 5A); however, in these areas, we did observe expression of the neutral endopeptidase CD10 (Figure 5D), a protein that, in glomeruli of control mice, is strongly expressed on PEC (Figure 5C).

Characterization of ECM

The composition of the ECM that is present in the adhesions was studied by staining serial sections with antibodies directed

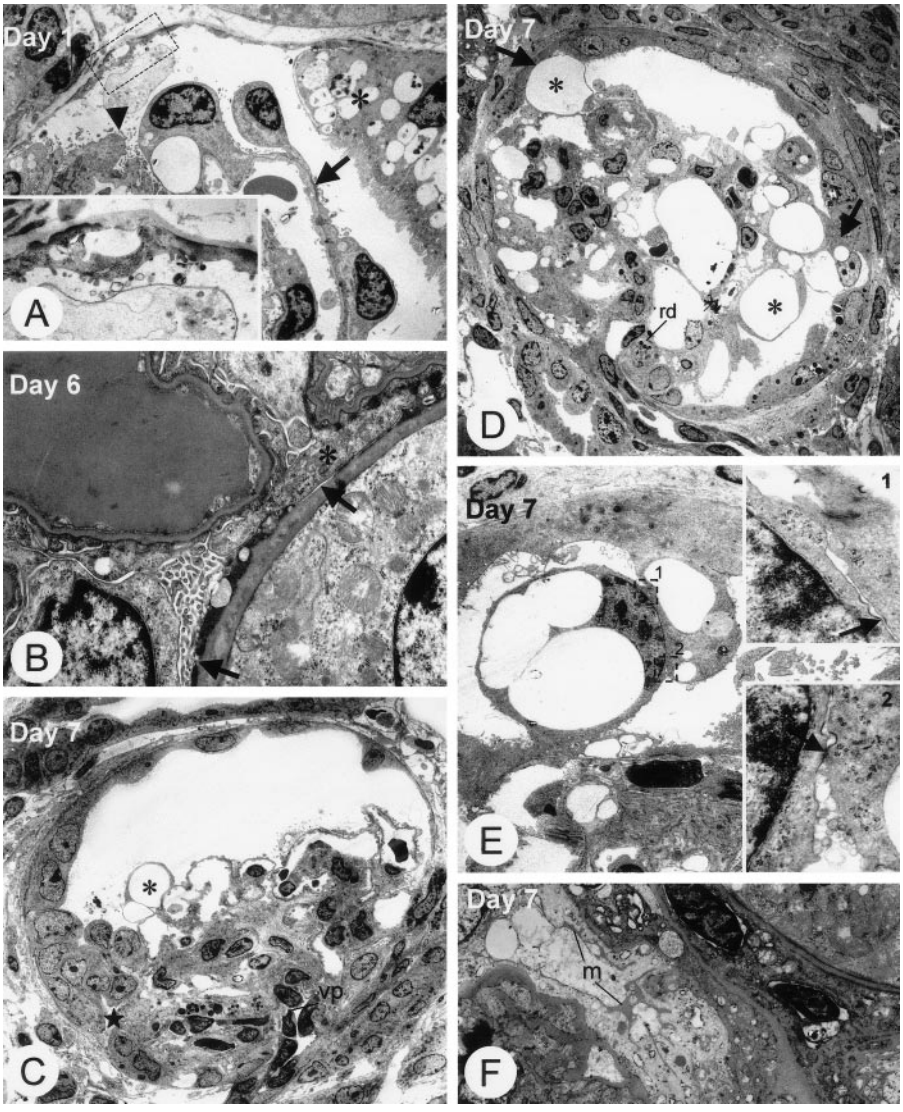

Figure 2. Electron microscopy. Injured glomeruli (days 1, 6, and 7) analyzed by transmission electron microscopy (TEM). (A) At day 1, PEC show widespread injury (insert). Epithelia of Bowman's capsule constituting proximal tubular epithelial cells show extensive vacuolization of the cytoplasm (*). Podocytes showed foot process effacement (arrow) and microvillous transformation (arrowhead). (B) At days 6 and 7, segments of denuded Bowman's capsule were observed (arrows). Podocytes positioned against the denuded capsule were observed, thus forming podocyte bridges between the GBM and the bare Bowman's capsule (*). (C-E) At days 6 and 7, in early lesions, PEC appeared activated with enlarged nuclei and prominent nucleoli. The number of PEC nuclei along Bowman's capsule appeared increased (★). The hyperplasia of epithelial cells in Bowman's space was also encountered near the vascular pole (vp). Podocytes were markedly hypertrophic showing extensive vacuolization, resorption droplets (rd), and formation of pseudocysts (*). In perfusion-fixed tissue, cell bridges formed by a hypertrophic podocyte attached to a PEC were observed (arrows). At the site of attachment between hypertrophic podocytes and PEC junctional complexes were occasionally observed (arrows in inserts 1 and 2). (F) Glomerular epithelial cells positioned in Bowman's space showed pericellular accumulation of ECM (m). (A, B, and F: immersion-fixed; C-E: perfusion-fixed) Original magnifications: A, ×1500; insert, ×3000; B, ×7500; C, ×600; D, ×500; E, ×1000; insert 1, ×12,000; insert 2, ×20 000; F, ×4000.

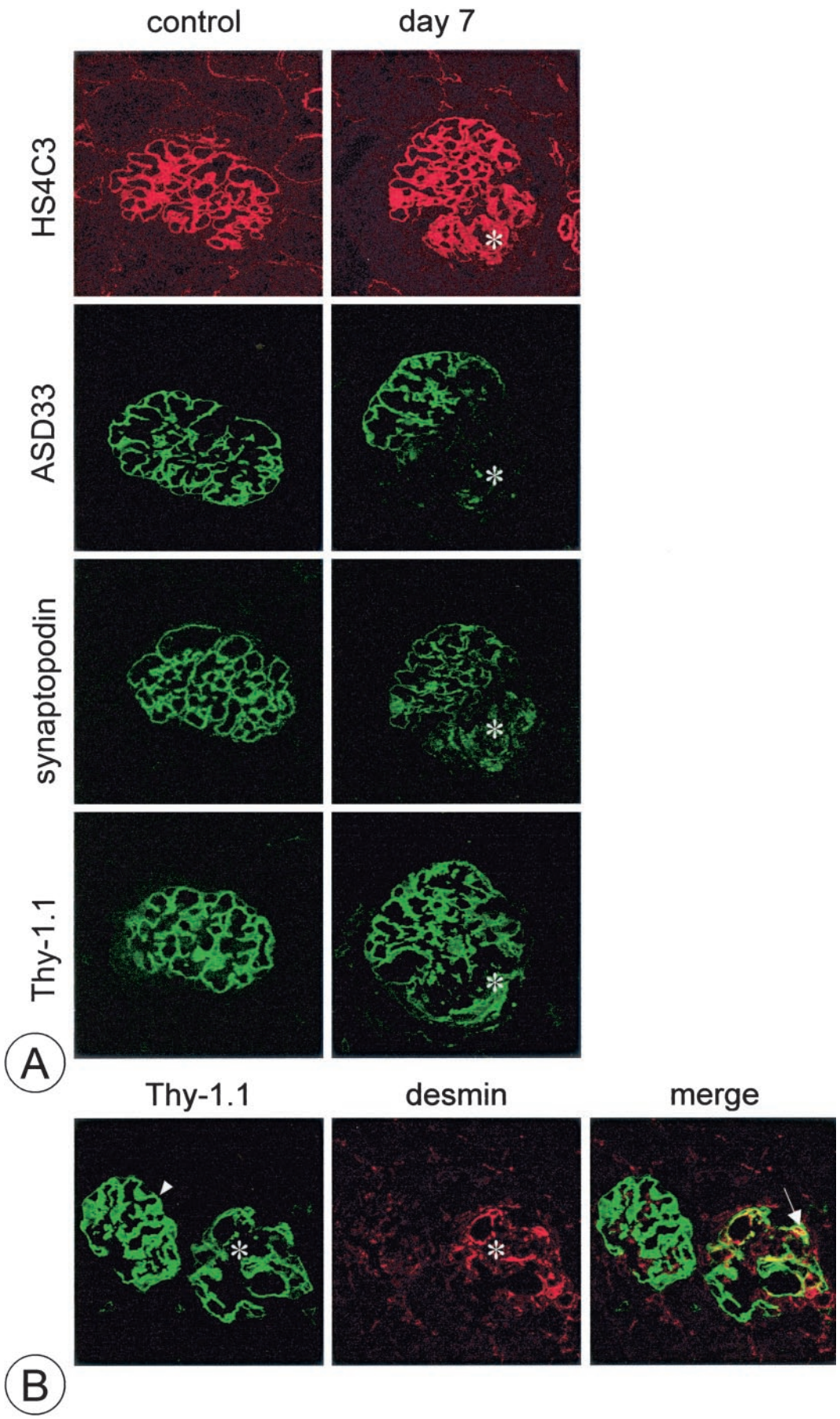

Figure 3. Podocyte phenotype. (A) Immunofluorescence for podocyte markers (ASD33, synaptopodin, Thy-1.1) and an anti-heparan sulfate single chain antibody (HS4C3). Serial sections, from control and anti-Thy-1.1 mAb–injected mice (day 7). HS4C3 stains GBM and mesangium, showing normal tuft architecture in the control and a segmental lesion in Thy-1.1–injected mice (day 7, *). In control mice, ASD33, synaptopodin, and Thy-1.1 showed a homogeneous staining pattern along the GBM. There is a decrease in expression of ASD33 and synaptopodin in areas with a segmental lesion. There is still high expression of the Thy-1.1 antigen surrounding the collapsed segment (arrow). (B) IF for desmin and Thy-1.1. Section from an anti-Thy-1.1 mAb–injected mouse (day 7). Thy-1.1 shows a normal podocyte staining in the unaffected glomerulus (arrowhead) but an irregular pattern in an affected glomerulus (*). The affected glomerulus shows expression of desmin (*). Desmin and Thy-1.1 colocalize in the affected glomerulus (arrow). Original magnification, ×500.

Table 2. Number of WT-1–positive cells per mm^2 in Thy-1.1 tg mice at different days after anti-Thy-1.1 mAb injection and in saline injected mice[a]

Group	WT-1–Positive Cells/mm^2	*n*
Saline	2388 ± 69	4
Day 1	2518 ± 169	5
Day 3	2497 ± 122	4
Day 6	2728 ± 81	4
Day 7	2332 ± 247	4
Day 10	2137 ± 412	3
Day 14	1974 ± 72	4
Day 21	1694 ± 141[b,c]	4

[a] In the first 7 d, there is no significant decrease in WT-1–positive cells *versus* the saline-injected mice. There is a significant decrease in number of WT-1–positive cells visible at day 21 *versus* day 1 and 6.
[b] $P < 0.05$ *versus* day 1.
[c] $P < 0.01$ *versus* day 6.

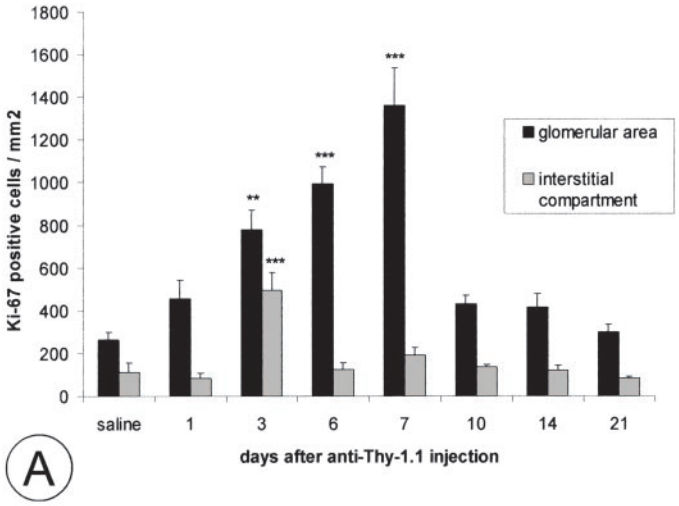

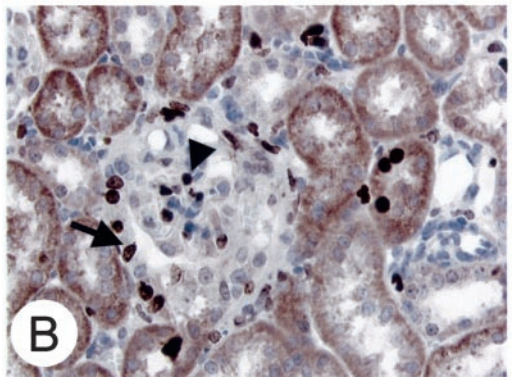

Figure 4. Cellular proliferation in the glomerulus and interstitial compartment. (A) The number of Ki-67–positive proliferating cells in the glomerulus gradually increased and peaked at day 7. Thereafter, the number of Ki-67–positive cells declined to baseline levels. Peak proliferation of cells within the interstitial compartment was observed at day 3. (B) Immunohistochemistry for Ki-76. Immunoreactive nuclei stain brown. There is a high number of Ki-67–positive cells positioned along Bowman's capsule (arrow). We also observed Ki-67 positive cells (arrowhead) within the glomerular tuft. Original magnification, ×400; $n = 4$; ** $P < 0.01$ *versus* saline; *** $P < 0.001$ *versus* saline.

against the α2 and α4 chains of collagen IV. In addition, we have used different anti-HS single chain antibodies that in control mice predominantly stain Bowman's capsule and not the GBM. The ECM forming tuft adhesions stained for collagen α2 (IV) and the anti-HS antibodies and were negative for collagen α4 (IV) and HS4C3, an anti-HS antibody that stains GBM and mesangium. Thus, the staining properties of the newly formed ECM were identical to those of Bowman's capsule, arguing that this matrix was produced by PEC rather than podocytes (Figure 6).

Discussion

Our study indicates that PEC play an important role in the development of FSGS in the Thy-1.1 tg mouse. Although we also observed distinct changes in the podocyte, we think that the involvement of the PEC is more prominent. In the early time points after induction of albuminuria, we observed PEC injury, which was accompanied by denudation of segments of the Bowman's capsule. Thereafter, a cellular lesion consisting of hypertrophic and hyperplastic glomerular epithelial cells developed. Although hypertrophic podocytes contributed to these lesions, most cells were proliferating PEC. Finally, the cellular lesions turned into the adhesive scar that is the hallmark of FSGS. We have evaluated the composition of the scar using antibodies against heparan sulfates and collagen (IV) α2 and α4, and the data indicated that the ECM that is present in the scar is derived from the parietal epithelium.

Podocyte changes in our model consisted of podocyte hypertrophy and podocyte foot process effacement. Of note, we never observed detachment of the podocytes or areas of denuded GBM. Our findings are in contrast with the observations of Kriz *et al.*, who have postulated a final common pathway for the development of FSGS on the basis of their studies in various rat models. Their proposed pathway toward FSGS emphasizes the podocyte. Detailed histologic analyses have pointed to the following sequence of events: (*1*) podocyte injury; (*2*) detachment of podocytes and/or loss of podocytes (podocytopenia) with denudation of the GBM; (*3*) adherence of the naked GBM to PEC, which then lose intercellular contacts; and (*4*) the formation of an adhesion between the glomerular tuft and Bowman's capsule, which allows "misdirected" filtration of plasma proteins to the periglomerular and peritubular space, ultimately leading to global glomerulosclerosis and tubulointerstitial fibrosis (13–17).

In our model, development of FSGS clearly follows other pathways, thus suggesting that the model proposed by Kriz *et al.* may not be applicable to FSGS in general. The latter conclusion may not come as a surprise in view of the large clinical variability of patients with FSGS. Thus far, most studies have been done in rat models with evidence of glomerular or systemic hypertension. Most notable is the observation

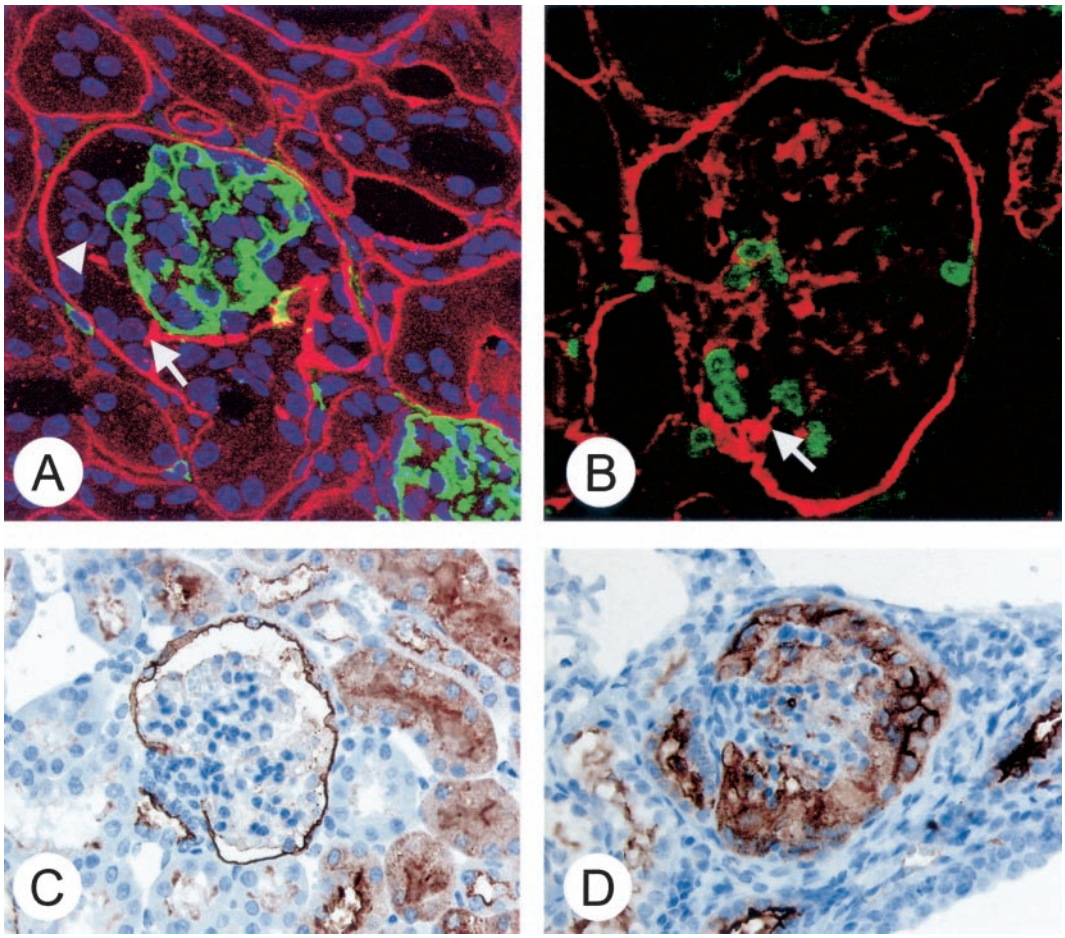

Figure 5. Phenotype of proliferating cells. Panel A shows immunofluorescence in an anti-Thy-1.1 mAb–injected mouse (day 7), for Thy-1.1 (green) and HS4E4, an anti-heparan sulfate antibody (red). Nuclei are stained with TO-PRO-3 (blue staining). Shown is a FSGS lesion with accumulation of cells in Bowman's space (A, arrowhead). Thy-1.1 is present along the glomerular tuft, but there is no staining for Thy-1.1 within the lesion. HS4E4 stains Bowman's capsule and tuft adhesions (A, arrow). Panel B shows immunofluorescence for collagen α2 (IV) (red) and Ki-67 (green). Collagen α2 (IV) is present in Bowman's capsule, mesangium, and tuft adhesions (B, arrow); Ki-67–positive cells are located adjacent to tuft adhesions. Magnifications: A, $\times$500; B, $\times$600. Panels C and D show immunohistochemistry for CD10. Immunoreactive cells stain brown. In control mice, CD10 is strongly expressed on PEC within the glomerulus (C). In a FSGS lesion (day 7), epithelial cells in Bowman's space strongly express CD10 (D). Original magnification, $\times$400.

that in the reported studies there was always evidence of capillary ballooning and glomerular hypertrophy. It is tempting to speculate that the proposed pathway toward FSGS based on the rat models is relevant for the process of secondary FSGS that is observed in patients with reduced renal mass or long-standing hypertension.

In our mouse model, we did not observe dilation of the glomerular capillaries or glomerular hypertrophy. Rather, we observed segmental collapse of the tuft with prominent extracapillary proliferation and frequent formation of adhesions. Therefore, from a morphologic point of view, the lesions in our mouse model closely resemble the collapsing variant of human FSGS (2,27), although the segmental rather than global nature of the process and the frequent formation of adhesions are more typical for other variants of human FSGS. Collapsing FSGS is a recently recognized entity, predominantly seen in African Americans, also associated with HIV infection, and with a poor prognosis and rapid progression toward end-stage renal disease (ESRD). Collapsing FSGS in humans is associated with higher initial proteinuria and by some authors considered to be early and/or active lesions (29–33). To what extent is our model representative of human collapsing FSGS? Kriz *et al.* consider collapsing FSGS to be distinct from the classical form, with a different underlying pathogenetic mechanism (14,15). It has been proposed that the cellular lesions that are prominently present in collapsing FSGS consist of podocytes that are dysregulated and are dedifferentiated with loss of all podocyte-specific markers (34–37) and increased expression of desmin (28). These podocytes are apparently no longer growth restricted and have regained the ability to proliferate. Normal podocytes are considered post-mitotic cells, unable to proliferate due to high-level expression of cyclin-dependent kinase inhibitors (CKI) p27 and p57 (34). In our mouse model, we also observed podocyte hypertrophy and loss of podocyte-specific markers, synaptopodin and ASD33, and an increased expression of desmin, consistent with dedifferen-

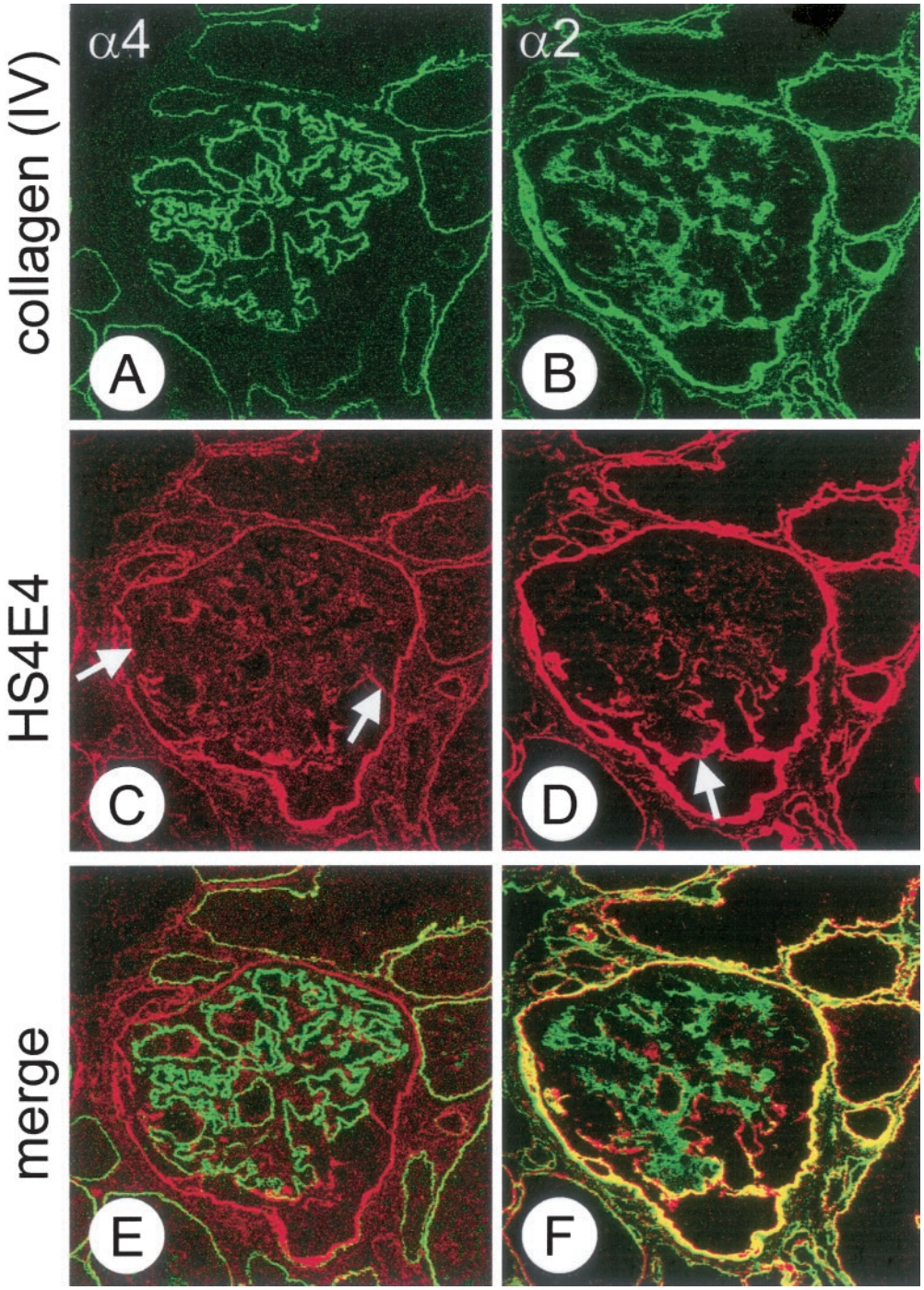

Figure 6. Assessment of the composition of the ECM. Immunofluorescence for collagen IV α2 and α4 (green) and HS4E4 (red) in serial sections of a glomerulus with adhesions (day 7). (A) Within the glomerulus, collagen α4 (IV) is expressed specifically in the GBM. (B) Collagen α2 (IV) is expressed in Bowman's capsule, mesangium, and the tuft adhesions. (C and D) HS4E4 stains Bowman's capsule and the accumulations of ECM, which form the tuft adhesions (arrows). (E) There was no co-localization of collagen α4 (IV) and heparan sulfate identified by HS4E4. (F) Collagen α2 (IV) shows co-localization with the HS4E4 heparan sulfate in Bowman's capsule and the tuft adhesions. Original magnification, ×500.

tiation. However, because of the continued expression of podocyte-specific markers, WT-1 and Thy-1.1, we were able to show that podocytes in our model do not proliferate. Conversely, the orientation of the proliferating epithelial cells relative to Bowman's capsule and Bowman's space, the strong expression of CD10 and the composition of the ECM that is produced by these cells strongly argue that the proliferating cells are PEC. PEC have low-level expression of CKI and are known to proliferate in response to different stimuli (38). A typical example of PEC proliferation is seen in the formation of crescents (39,40). Taken together, our data argue against a dedifferentiated and dysregulated podocyte being responsible for the formation of FSGS lesions in our model.

How should earlier data be interpreted? In the studies that have assessed podocyte dedifferentiation, it is noteworthy that these "dedifferentiated podocytes" had lost expression of WT-1, GLEPP, synaptopodin, and podocalyxin. Some cells had detached from the GBM, and these cells did not express podocyte markers but rather demonstrated characteristic features of macrophages (41,42). Thus, it cannot be excluded that some of the cells present in cellular lesions in human collapsing FSGS originate from proliferating PEC. Contribution of

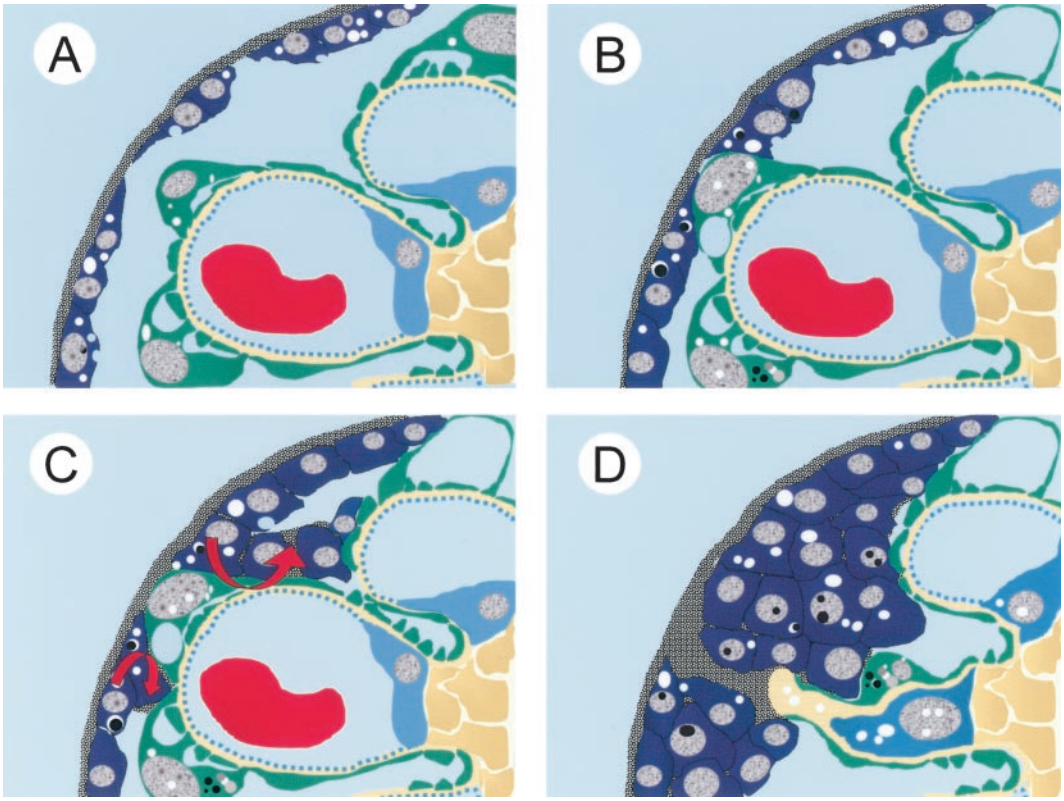

Figure 7. Hypothetical sequence of events leading to cellular FSGS lesions in the Thy1.1 tg mice, illustrated in schematic drawings. (A) Days 1–7. Injury of the glomerular epithelial cells. Podocytes (green) show foot process effacement and microvillous transformation (not illustrated). There is no podocyte detachment. PEC (blue) show vacuolization and detachment, leading to "bare" segments of Bowman's capsule (Bowman's capsule is drawn as a gray line). (B) Days 3–7. Podocytes become hypertrophic (with activated nuclei, resorption droplets, and pseudocysts) and form bridges between the glomerular tuft and Bowman's capsule. (C) Days 6 and 7. Proliferation of PEC adjacent to the bridging podocytes, filling up Bowman's space, giving the appearance of a cellular FSGS lesion. (D) The proliferating PEC in Bowman's space produce ECM (gray) that eventually forms tuft adhesions.

PEC to cellular lesions in human collapsing FSGS has been previously proposed by other authors on the basis of positive staining for cytokeratin (38). We also need to consider the possibility that FSGS lesions may develop differently in mouse as compared with humans. In mouse glomeruli, proximal tubular epithelial cells are present within the glomerulus close to the urinary pole. It cannot be excluded that proximal tubular epithelial cells proliferate and influence FSGS development. The fact that in our mice FSGS lesions develop not only close to the urinary pole but also in the perihilar region argues against this possibility. Nevertheless, the existence of proximal tubular epithelial cells within Bowman's capsule in mice complicates any analysis of glomerular cell changes.

The finding that cellular lesions in our model are of PEC origin does not preclude an important role for the podocyte in the development of FSGS lesions. The initial bridge consists of a hypertrophic podocyte that attaches to PEC or comes into contact with Bowman's capsule. Attachment of a hypertrophic podocyte to PEC or appositioning to denuded Bowman's capsule may be the critical event that leads to an FSGS lesion. In this respect, our findings partly resemble crescent formation in a mouse model of crescentic glomerulonephritis (39). These authors observed that podocyte bridges between the capillary tuft and Bowman's capsule precede the development of crescents. In this model, PEC injury with gaps between the PEC and areas of denuded Bowman's capsule was not observed. The authors suggest that the bridging podocyte is critically involved in regulating proliferation of PEC. In our model, a similar effect may then be responsible for the proliferation of the PEC that we observed. Le Hir *et al.* (39) suggests that the podocyte produced basement membrane-like material that formed in continuity with the Bowman's capsule. However, this conclusion was based on staining for collagen IV with a polyclonal antibody, which does not allow differentiation between different α-chains. Our findings clearly prove that the adhesion is made up of Bowman's capsule like material. In Figure 7, we have proposed a scheme for the sequence of events that ultimately lead to FSGS in our model.

How to reconcile both models with human data? As mentioned above, the classical pathway of FSGS as described by Kriz *et al.* in rat models of hypertrophy and hypertension may best fit with secondary FSGS. Our model may bear more resemblance to primary FSGS. This needs to be further investigated using human renal biopsy material. Notably, PEC damage in biopsies from patients with FSGS is frequently observed (43–45) and possibly caused by protein overload.

In conclusion, PEC play an important role in the formation of cellular FSGS lesions in the Thy-1.1 tg mouse.

Acknowledgments

This work was supported by a grant from the Dutch Kidney Foundation (C 99.1844). We thank Dr. Yoshikazu Sado (Shigei Medical Research Institute, Okayama, Japan) for providing the anti-collagen IV α2 and α4 antibodies.

References

1. Haas M, Meehan SM, Karrison TG, Spargo BH: Changing etiologies of unexplained adult nephrotic syndrome: a comparison of renal biopsy findings from 1976–1979 and 1995–1997. *Am J Kidney Dis* 30: 621–631, 1997
2. D'Agati V: The many masks of focal segmental glomerulosclerosis. *Kidney Int* 46: 1223–1241, 1994
3. Cameron JS: The enigma of focal segmental glomerulosclerosis. *Kidney Int Suppl* 57: S119–S131, 1996
4. Kashgarian M, Sterzel RB: The pathobiology of the mesangium. *Kidney Int* 41: 524–529, 1992
5. Striker LJ, Doi T, Elliot S, Striker GE: The contribution of glomerular mesangial cells to progressive glomerulosclerosis. *Semin Nephrol* 9: 318–328, 1989
6. Floege J, Alpers CE, Burns MW, Pritzl P, Gordon K, Couser WG, Johnson RJ: Glomerular cells, extracellular matrix accumulation, and the development of glomerulosclerosis in the remnant kidney model. *Lab Invest* 66: 485–497, 1992
7. Jacobson HR: Chronic renal failure: pathophysiology. *Lancet* 338: 419–423, 1991
8. Kretzler M, Koeppen-Hagemann I, Kriz W: Podocyte damage is a critical step in the development of glomerulosclerosis in the uninephrectomised-desoxycorticosterone hypertensive rat. *Virchows Arch* 425: 181–193, 1994
9. Kriz W, Hosser H, Hahnel B, Simons JL, Provoost AP: Development of vascular pole-associated glomerulosclerosis in the Fawn-hooded rat. *J Am Soc Nephrol* 9: 381–396, 1998
10. Kriz W, Hahnel B, Rosener S, Elger M: Long-term treatment of rats with FGF-2 results in focal segmental glomerulosclerosis. *Kidney Int* 48: 1435–1450, 1995
11. Kriz W, Kretzler M, Nagata M, Provoost AP, Shirato I, Uiker S, Sakai T, Lemley KV: A frequent pathway to glomerulosclerosis: deterioration of tuft architecture-podocyte damage-segmental sclerosis. *Kidney Blood Press Res* 19: 245–253, 1996
12. Nagata M, Kriz W: Glomerular damage after uninephrectomy in young rats. II. Mechanical stress on podocytes as a pathway to sclerosis. *Kidney Int* 42: 148–160, 1992
13. Kriz W, Elger M, Hosser H, Hahnel B, Provoost A, Kranzlin B, Gretz N: How does podocyte damage result in tubular damage? *Kidney Blood Press Res* 22: 26–36, 1999
14. Kriz W, Lemley KV: The role of the podocyte in glomerulosclerosis. *Curr Opin Nephrol Hypertens* 8: 489–497, 1999
15. Kriz W, Gretz N, Lemley KV: Progression of glomerular diseases: is the podocyte the culprit? *Kidney Int* 54: 687–697, 1998
16. Kriz W, Hartmann I, Hosser H, Hahnel B, Kranzlin B, Provoost A, Gretz N: Tracer studies in the rat demonstrate misdirected filtration and peritubular filtrate spreading in nephrons with segmental glomerulosclerosis. *J Am Soc Nephrol* 12: 496–506, 2001
17. Kriz W, Elger M, Nagata M, Kretzler M, Uiker S, Koeppen-Hageman I, Tenschert S, Lemley KV: The role of podocytes in the development of glomerular sclerosis. *Kidney Int Suppl* 45: S64–S72, 1994
18. Assmann KJ, van Son JP, Dijkman HB, Mentzel S, Wetzels JF: Antibody-induced albuminuria and accelerated focal glomerulosclerosis in the Thy-1.1 transgenic mouse. *Kidney Int* 62: 116–126, 2002
19. Smeets B, Dijkman HB, Te Loeke NA, van Son JP, Steenbergen EJ, Assmann KJ, Wetzels JF, Groenen PJ: Podocyte changes upon induction of albuminuria in Thy-1.1 transgenic mice. Nephrol. Dial. Transplant 18: 2524–2533, 2003
20. Kollias G, Evans DJ, Ritter M, Beech J, Morris R, Grosveld F: Ectopic expression of Thy-1 in the kidneys of transgenic mice induces functional and proliferative abnormalities. *Cell* 51: 21–31, 1987
21. Assmann KJ, Tangelder MM, Lange WP, Tadema TM, Koene RA: Membranous glomerulonephritis in the mouse. *Kidney Int* 24: 303–312, 1983
22. Ramaekers FC, Moesker O, Huysmans A, Schaart G, Westerhof G, Wagenaar SS, Herman CJ, Vooijs GP: Intermediate filament proteins in the study of tumor heterogeneity: an in-depth study of tumors of the urinary and respiratory tracts. *Ann N Y Acad Sci* 455: 614–634, 1985
23. Lostrom ME, Stone MR, Tam M, Burnette WN, Pinter A, Nowinski RC: Monoclonal antibodies against murine leukemia viruses: identification of six antigenic determinants on the p 15(E) and gp70 envelope proteins. *Virology* 98: 336–350, 1979
24. Mentzel S, van Son JP, De Jong AS, Dijkman HB, Koene RA, Wetzels JF, Assmann KJ: Mouse glomerular epithelial cells in culture with features of podocytes in vivo express aminopeptidase A and angiotensinogen but not other components of the renin-angiotensin system. *J Am Soc Nephrol* 8: 706–719, 1997
25. van Kuppevelt TH, Dennissen MA, van Venrooij WJ, Hoet RM, Veerkamp JH: Generation and application of type-specific anti-heparan sulfate antibodies using phage display technology. Further evidence for heparan sulfate heterogeneity in the kidney. *J Biol Chem* 273: 12960–12966, 1998
26. Dennissen MA, Jenniskens GJ, Pieffers M, Versteeg EM, Petitou M, Veerkamp JH, van Kuppevelt TH: Large, tissue-regulated domain diversity of heparan sulfates demonstrated by phage display antibodies. *J Biol Chem* 277: 10982–10986, 2002
27. D'Agati V: Pathologic classification of focal segmental glomerulosclerosis. *Semin Nephrol* 23: 117–134, 2003
28. Barisoni L, Bruggeman LA, Mundel P, D'Agati VD, Klotman PE: HIV-1 induces renal epithelial dedifferentiation in a transgenic model of HIV-associated nephropathy. *Kidney Int* 58: 173–181, 2000
29. Weiss MA, Daquioag E, Margolin EG, Pollak VE: Nephrotic syndrome, progressive irreversible renal failure, and glomerular "collapse": A new clinicopathologic entity? *Am J Kidney Dis* 7: 20–28, 1986
30. Schwartz MM, Lewis EJ: Focal segmental glomerular sclerosis: The cellular lesion. *Kidney Int* 28: 968–974, 1985
31. Schwartz MM, Evans J, Bain R, Korbet SM: Focal segmental glomerulosclerosis: prognostic implications of the cellular lesion. *J Am Soc Nephrol* 10: 1900–1907, 1999
32. Detwiler RK, Falk RJ, Hogan SL, Jennette JC: Collapsing glomerulopathy: a clinically and pathologically distinct variant of focal segmental glomerulosclerosis. *Kidney Int* 45: 1416–1424, 1994
33. Valeri A, Barisoni L, Appel GB, Seigle R, D'Agati V: Idiopathic collapsing focal segmental glomerulosclerosis: a clinicopathologic study. *Kidney Int* 50: 1734–1746, 1996

34. Barisoni L, Mokrzycki M, Sablay L, Nagata M, Yamase H, Mundel P: Podocyte cell cycle regulation and proliferation in collapsing glomerulopathies. *Kidney Int* 58: 137–143, 2000
35. Barisoni L, Kopp JB: Modulation of podocyte phenotype in collapsing glomerulopathies. *Microsc Res Tech* 57: 254–262, 2002
36. Yang Y, Gubler MC, Beaufils H: Dysregulation of podocyte phenotype in idiopathic collapsing glomerulopathy and HIV-associated nephropathy. *Nephron* 91: 416–423, 2002
37. Barisoni L, Kriz W, Mundel P, D'Agati V: The dysregulated podocyte phenotype: a novel concept in the pathogenesis of collapsing idiopathic focal segmental glomerulosclerosis and HIV-associated nephropathy. *J Am Soc Nephrol* 10: 51–61, 1999
38. Nagata M, Horita S, Shu Y, Shibata S, Hattori M, Ito K, Watanabe T: Phenotypic characteristics and cyclin-dependent kinase inhibitors repression in hyperplastic epithelial pathology in idiopathic focal segmental glomerulosclerosis. *Lab Invest* 80: 869–880, 2000
39. Le Hir ML, Keller C, Eschmann V, Hahnel B, Hosser H, Kriz W: Podocyte bridges between the Tuft and Bowman's Capsule: An early event in experimental crescentic glomerulonephritis. *J Am Soc Nephrol* 12: 2060–2071, 2001
40. Nitta K, Horita S, Honda K, Uchida K, Watanabe T, Nihei H, Nagata M: Glomerular expression of cell-cycle-regulatory proteins in human crescentic glomerulonephritis. *Virchows Arch* 435: 422–427, 1999
41. Bariety J, Bruneval P, Hill G, Irinopoulou T, Mandet C, Meyrier A: Posttransplantation relapse of FSGS is characterized by glomerular epithelial cell transdifferentiation. *J Am Soc Nephrol* 12: 261–274, 2001
42. Bariety J, Nochy D, Mandet C, Jacquot C, Glotz D, Meyrier A: Podocytes undergo phenotypic changes and express macrophagic-associated markers in idiopathic collapsing glomerulopathy. *Kidney Int* 53: 918–925, 1998
43. Van Damme B, Tardanico R, Vanrenterghem Y, Desmet V: Adhesions, focal sclerosis, protein crescents, and capsular lesions in membranous nephropathy. *J Pathol* 161: 47–56, 1990
44. Gaffney EF: Prominent parietal epithelium: a common sign of renal glomerular injury. *Hum Pathol* 13: 651–660, 1982
45. Gaffney EF, Panner BJ: Membranous glomerulonephritis: clinical significance of glomerular hypercellularity and parietal epithelial abnormalities. *Nephron* 29: 209–215, 1981